

# Enabling Storage Class Memory as a DRAM Replacement for Datacenter Services

Dmitrii Ustiugov  
EcoCloud, EPFL  
dmitrii.ustiugov@epfl.ch

Alexandros Daglis  
EcoCloud, EPFL  
alexandros.daglis@epfl.ch

Javier Picorel  
Huawei  
javier.picorel@huawei.com

Mark Sutherland  
EcoCloud, EPFL  
mark.sutherland@epfl.ch

Babak Falsafi  
EcoCloud, EPFL  
babak.falsafi@epfl.ch

Edouard Bugnion  
EcoCloud, EPFL  
edouard.bugnion@epfl.ch

Dionisios Pnevmatikatos  
FORTH-ICS & ECE-TUC  
pnevmati@ics.forth.gr

## ABSTRACT

With emerging storage-class memory (SCM) nearing commercialization, there is evidence that it will deliver the much-anticipated high density and access latencies within only a few factors of DRAM. Nevertheless, the latency-sensitive nature of memory-resident services makes seamless integration of SCM in servers questionable. In this paper, we ask the question of how best to introduce SCM for such servers to improve overall performance/cost over existing DRAM-only architectures. We first show that even with the most optimistic latency projections for SCM, the higher memory access latency results in prohibitive performance degradation. However, we find that deployment of a modestly sized high-bandwidth 3D stacked DRAM cache makes the performance of an SCM-mostly memory system competitive. The high degree of spatial locality that memory-resident services exhibit not only simplifies the DRAM cache’s design as page-based, but also enables the amortization of increased SCM access latencies and the mitigation of SCM’s read/write latency disparity.

We identify the set of memory hierarchy design parameters that plays a key role in the performance and cost of a memory system combining an SCM technology and a 3D stacked DRAM cache. We then introduce a methodology to drive provisioning for each of these design parameters under a target performance/cost goal. Finally, we use our methodology to derive concrete results for specific SCM technologies. With PCM as a case study, we show that a two bits/cell technology hits the performance/cost sweet spot, reducing the memory subsystem cost by 40% while keeping performance within 3% of the best performing DRAM-only system, whereas single-level and triple-level cell organizations are impractical for use as memory replacements.

## 1 INTRODUCTION

For almost 50 years, DRAM has served as the universal standard for memory in mainframes, laptops, and today’s datacenters. In the datacenter, however, we are entering a new age where memory will no longer exclusively be comprised of DRAM. Although the interactive nature of online services will continue to dictate that hot data must be kept DRAM resident, capacity limitations have begun to pressure datacenter operators to investigate emerging technologies to eventually replace it. Future servers will undoubtedly retain

some DRAM for performance optimization, while shifting to denser main memory to hold vast modern datasets.

As dataset sizes have continued marching upwards in their exponential growth trend [2], datacenter operators and memory architects have been unable to keep pace, obstructed by fundamental limitations on channels per packaged IC as well as intra-channel signal integrity. With the pressure squarely on DRAM manufacturers to deliver DIMMs with ever-increasing capacities, memory has begun to form a significant fraction of server acquisition cost<sup>1</sup>, as high density components command higher margins and therefore prices. The synthesis of these two trends has led to a concerted effort to provision memory systems with reduced cost per bit, markedly reducing expenditure for large volume deployments.

Emerging storage-class memory (SCM) technologies are a prime candidate to serve as the next generation of main memory, as they boast approximately an order of magnitude greater density than DRAM at a lower cost per bit [29, 60, 72, 83]. These traits come at the price of increased access latency when compared to commodity DRAM, creating new challenges for systems designers as memory latency is a critical factor in datacenter application performance [37]. Given that typical SCM latencies are 4–100× higher than DRAM [65, 71], naïvely and completely replacing DRAM with SCM is an unacceptable compromise for datacenter operators.

In addition to the self-evident latency problem, SCM devices come in many flavors, with typically inverse relationships between latency and density—denser devices typically yield lower cost per bit but are slower. This variety presents a challenge to system designers: ideally, one would like to use the cheapest, highest capacity devices, but those will degrade performance the most. In this paper, we identify an opportunity to significantly improve the performance of emerging SCM devices, aided by the insight that the elevated latencies required to access the slower data arrays can be amortized with bulk accesses; our solution proposes a hierarchical memory system that preserves performance while reducing cost.

Our memory system replaces conventional DRAM with a two-tier hierarchy, combining high-density SCM with a modestly sized 3D stacked DRAM cache; the former component offers cheap capacity and reduced cost, while the latter preserves the low latency and

<sup>1</sup>With a commodity Xeon E5-2660 v4 CPU and 256GB of DRAM, the memory represents up to 40% of the server’s total acquisition cost [17, 48].

high bandwidth required to ensure interactivity for online services. The structure of our hierarchy is informed by the insight that SCM’s longer access latencies can be amortized by bulk accesses; therefore we show that the stacked DRAM cache is best organized with page-size blocks whose sizes match with the SCM’s row buffer. Using a 3D stacked DRAM cache aggregates the application’s fine-grained accesses while a block is cache-resident, creating bulk transfers to and from the SCM and therefore amortizing its latency.

Figure 1a is a block diagram of our proposed SCM hierarchy. We show that by carefully provisioning both levels, datacenter operators can reduce the memory system’s total cost by 40% while maintaining performance within 3% of the best performing DRAM-based system.

The plurality of available SCM and 3D stacked DRAM devices complicates designing such a memory hierarchy. A system designer will be faced with choices pertaining to SCM latency, capacity, memory technology, and form factor; on the 3D stacked DRAM cache side, its high design and integration costs [15] diminish the returns in cost/bit attained by replacing DRAM with SCM, requiring designers to be judicious in choosing its parameters (e.g., capacity and block size). Hence, the design space for two-level hierarchies is extremely broad, spanning wide performance and cost ranges.

To guide system designers through this complex design space, we devise a design exploration methodology for different SCM technologies. Our methodology operates as follows: based on our insight that SCM latencies can be amortized with bulk transfers, we identify the key design parameter for any SCM device as its *row buffer size*, which sets the upper bound on the transfer size to/from the backing data array. For that given row buffer size, we bound the maximum acceptable SCM *read* and *write latencies* (thus, implicitly, the minimum SCM device cost), that preserve application performance. We frame these three parameters as a volume, where all SCM devices falling inside the volume are acceptable choices; an example of this design volume is shown in Figure 1b. Our methodology allows designers to pinpoint the most cost-effective hierarchies that still meet application performance targets.

To summarize, our main contributions are the following:

- We analyze emerging SCM devices being packaged in a DIMM form factor, and conclusively show that even the fastest among them cannot directly replace DRAM due to their long access latencies.
- We show that end-to-end performance of DRAM-based servers can be maintained by provisioning SCM-based main memory coupled with a modestly sized DRAM cache. We leverage the immense internal memory-level parallelism of 3D stacked technology to cope with the high bandwidth demands placed on the cache, while page-based cache organization enables amortization of SCM’s high access latency via bulk data transfers.
- We identify the set of key design parameters for hybrid SCM-DRAM memory hierarchies, then devise a methodology to prune the vast design space and identify SCM device configurations that offer the highest density, while maintaining performance close to the best performing DRAM-only memory hierarchy. Interestingly, we find that the right combination of SCM row buffer and DRAM cache sizing obviates

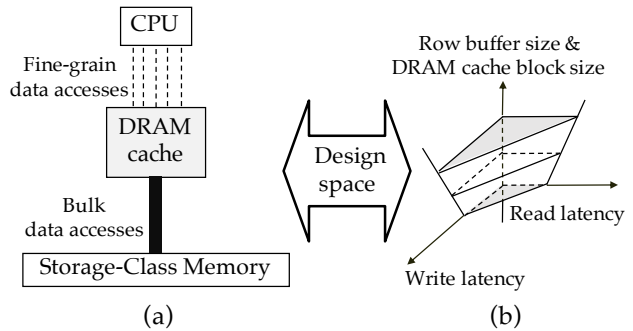


Figure 1: SCM hierarchy and design space exploration methodology.

all performance concerns related to the read/write latency disparity inherent in SCM technologies.

- We apply our methodology to conduct a case study on emerging phase-change memory (PCM) devices for servers, and demonstrate that 2-bit cell organizations (MLC) represent the only cost-effective choice, while both 1-bit and 3-bit cells fail to introduce an appealing design point in terms of performance/cost. MLC-based memory hierarchies are up to 1.8× more cost-effective than their DRAM-based counterparts, while delivering comparable performance.

The rest of the paper is organized as follows: First, we describe emerging SCM technologies in §2 and motivate our insight to amortize SCM latency with bulk transfers. We then analyze server workloads in §3 to show that naïvely replacing SCM with DRAM is impractical without the use of a 3D stacked page-based DRAM cache, and identify the cache’s most suitable parameters. As said cache inflates the system’s cost, we introduce a design space exploration methodology in §4 to drive our search for cost-effective system configurations. Based on our evaluation methodology presented in §5, we provide sample parameters for the SCM design space for servers, and perform a case study with emerging phase-change memory in §6. We discuss additional relevant aspects of hybrid memory hierarchy design in §7 and related work in §8. Finally, §9 concludes.

## 2 SCM BACKGROUND

Storage-class memory (SCM) is a term that encapsulates a class of emerging and much-anticipated technologies that are expected to penetrate the computing market in the following decade [29, 41, 60]. Being slower and denser than DRAM, but faster than Flash while retaining persistence, it cannot be strictly classified as either memory or storage but has characteristics of both. While the first SCM products were marketed as faster block-based storage devices, memory vendors have recently announced the launch of SCMs packaged in a dual in-line memory module (DIMM) form factor and using the conventional DDR interface [29], with the ultimate goal of replacing DRAM as main memory. The latter usage of SCM will be far more disruptive for modern servers, as the increased density boasted by SCM devices will translate into a commensurate reduction in the cost of memory.

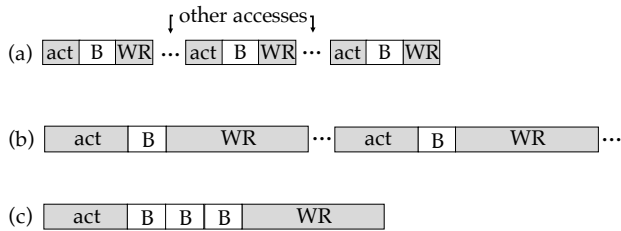


**Figure 2: Temporally batched bursts amortize activation cost.** *act*: activation, *B*: burst, *WR*: write restoration. (a) DRAM, (b) SCM, (c) SCM with batched bursts.

Although designing SCM DIMMs for compatibility by using the DDR interface will potentially accelerate their adoption, it also introduces performance disparities due to the fundamental differences in the underlying DRAM and SCM technologies. More specifically, the DDR interface specifies that the 64-bit wide channel is driven from a fast SRAM-based *row buffer*, which stores the most recently used row opened from the data array. Every access to the row buffer is referred to as a *burst*, where the requested word (64 bits) is selected from the row buffer and driven across the interface. The row buffer operates at the memory’s clock speed, the speed of which must remain consistent between SCM and DRAM DIMMs to ensure compatibility with today’s integrated memory controllers. Accessing an address that is not currently present in the row buffer (i.e., a row buffer miss) means that the existing row must be closed, and the proper row read into the buffer, which is referred to as an *activation*. Existing data that is dirty must be written back to the data array prior to opening the new row, in a process that is called *write restoration*.

Maintaining the same DDR interface and simply swapping the DRAM data array for SCM results in severe disparity between DDR channel speed and data array access latency: every row buffer miss now incurs between 4–100× the DRAM latency [65, 71] to read the SCM data array. Given this elevated disparity between the row buffer and data arrays, the bandwidth of modern SCM devices depends heavily on the fraction of accesses that hit in the row buffer.

Figure 2 graphically demonstrates this behavior, using an example of three write accesses either hitting or missing the same open row buffer. We use writes because clean rows do not incur write restorations in persistent memory. In Figure 2a and Figure 2b, we show the increase in total access latency that results from replacing a DRAM array with SCM. Although the burst latency remains the same (due to the standardized DDR interface), SCM’s increased array activation and write restoration latency now dominate the overall latency of the three write accesses. Figure 2c shows how the activation and restoration costs can be amortized when the three writes all hit in the open row, and then are written back together.

Motivated by the performance premium SCM DIMMs place on row buffer hits, we conduct an experiment to compare the average memory access time (AMAT) of a representative DRAM- and SCM-based DDR4-2666 DIMM with 8KB row buffers, varying the size of each memory request. Larger requests serve as a proxy for access

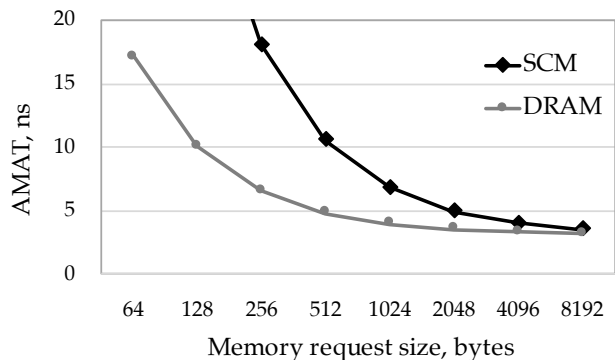


**Figure 3: AMAT as a function of transfer size (DRAM/SCM row activation time = 14ns/60ns).**

patterns that incur more hits in each opened row. We define AMAT as the average transfer latency of a cache block (64B) from memory to the CPU’s last-level cache and model an SCM array with 10× the read latency of DDR4 and 2× read/write disparity. Methodology details can be found in §5.

Figure 3 shows the results of this experiment. The DRAM’s latency quickly becomes bound by the channel’s speed, as the 14ns activation time is amortized with approximately 1KB of data transfer. In contrast, the SCM requires far larger requests to approach the DRAM’s AMAT, because of its significantly higher activation time of 60ns. Unfortunately, the access patterns of real applications are hardly so simple. We therefore conclude that directly replacing DRAM with SCM, using the same DDR interface, places the memory system’s performance entirely at the mercy of the applications’ access patterns, and whether or not they expose enough row buffer locality. In the next section, we study typical datacenter applications to determine if their memory access patterns result in the row buffer locality required by SCM DIMMs.

### 3 SCM HIERARCHY DESIGN FOR SERVERS

In this section, we investigate the feasibility of replacing a server’s DRAM with SCM. We find that direct replacement results in unacceptable performance degradation, but the use of a modestly sized 3D-stacked DRAM cache makes the replacement viable. Due to the high cost and complexity of such 3D caches, we conduct a detailed study to determine the most effective cache organization in terms of capacity, associativity, and block size.

#### 3.1 Workload compatibility with SCM

As memory latency is a critical performance determinant for datacenter workloads [23, 37], the dramatic increase in AMAT caused by replacing DRAM with SCM will directly manifest itself in end-to-end performance degradation. Therefore, we begin with an empirical study of representative server workloads, taken from the CloudSuite benchmarks [23], where we directly compare DRAM-based main memory against an SCM-based alternative and quantify the performance loss from simply replacing the memory technology.

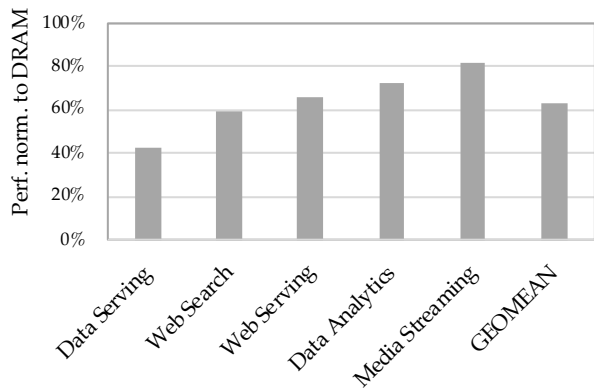


**Figure 4: SCM-based vs. DRAM-based memory (SCM Read/Write = 60ns/150ns).**

In this study, we choose to model an SCM device with latency-optimized characteristics to provide an upper bound on the performance of an SCM DIMM. Our application performance metric is the number of user-level instructions per cycle (U-IPC) retired by the server during our measurement intervals; U-IPC has been shown to accurately reflect server throughput [70]. For more details on our methodology, see §5.

Figure 4 shows the performance of server workloads with SCM-based main memory, normalized to the performance of a server using only DRAM. The results show that naively replacing DRAM with SCM results in a severe performance degradation of 37% on average. To identify whether or not the root cause of this performance degradation is the inflated latency of fine-grained accesses to the SCM (as explained in §2), we collect the row buffer hit ratio and the access percentage of each opened row (i.e., number of 64B chunks accessed by the CPU).

We find that 31% of memory accesses result in a row buffer hit on average, corroborating prior results [69]. Given that we modeled an 8KB row buffer (common in modern DRAM DIMMs [47]), a 31% hit ratio corresponds to an average of 2.6KB accessed per row buffer activation (i.e., consumed by the CPU before row closure). Our device model in Figure 3 shows that at this request size, an *unloaded* SCM device results in an AMAT 1.33× higher than DRAM. A *loaded* system with multiple outstanding requests is expected to have an even higher AMAT, as multiple outstanding requests may be forced to wait in the SCM’s command queues during activations or restorations, placing even more importance on maximizing row buffer hits. Indeed, in our experiments running full server workloads (Figure 4), we measure the AMAT on the SCM-based system to be 2.7× higher than its DRAM-based counterpart.

In the context of designing a server memory hierarchy using SCM, it is necessary to confirm that the workloads themselves actually have the potential to expose more row buffer locality; if so, a judicious organization of the memory system can immediately restore some of the lost performance. Prior work that has studied row buffer locality in scale-out workloads has reported that an ideal memory scheduling system can achieve row buffer hit ratios of 77% [69], a 2.5× increase over what we observe. The same work also

demonstrated abundant spatial locality present in the workloads themselves, with many pages incurring hits to over 50% of their constituent cache blocks during their lifetime in the LLC. Unfortunately, because the memory channels in a modern server processor are multiplexed between many CPU cores, interleaving their access streams destroys a large fraction of whatever row buffer locality would have existed, had the application executed in isolation [69].

Since our workloads indeed exhibit row buffer locality that can be harvested to address the concerns discussed in §2, we identify two key requirements for a server wishing to use SCM:

- (1) SCM devices place paramount importance on row buffer hits due to their slow backing data arrays.
- (2) Pages that are placed into the DIMM’s row buffers need to remain open for long periods of time, in order to collect all of the spatially local accesses, before write restoration occurs.

In the next section, we examine whether any feasible SCM device can meet these requirements.

### 3.2 Designing SCMs to meet key requirements

A naïve conclusion from our previous two observations would be that memory architects should build SCM DIMMs with large row buffers to improve the probability of hits, and further optimize memory scheduling to exploit spatial locality therein. However, the write programming process of various SCM technologies precludes us from constructing rows that are comparable in size to what currently exists in DRAM DIMMs (8KB), due to limitations on write current that can be driven into the data cells during the write restoration stage [26, 33]. Current SCM devices come with row buffer sizes in the 512–2048B range [39, 65]. Even with perfect spatial locality, these small rows do not provide enough opportunity to fully amortize the SCM’s higher latencies. This problem can once again be seen in Figure 3, where transfer sizes of 1KB and 2KB result in the SCM’s AMAT being elevated over DRAM by approximately 1.4× and 1.3×, respectively. Furthermore, techniques for row buffer optimization [64, 69] can only provide a maximum row buffer hit rate of 50%, which unfortunately lags far behind the hit rates required to guarantee application performance. These fundamental SCM limitations, combined with limited scheduling scope in the memory controllers, lead us to conclude that SCM cannot serve as a drop-in DRAM replacement.

Although we conclusively show that a server cannot use SCM alone as its main memory while preserving application performance, we emphasize that the motivations for using SCM are its capacity and low cost, not higher performance over DRAM. Therefore, we propose to learn from existing performance-maximizing solutions that can enable us to recoup some (ideally most) of the performance lost by replacing DRAM with SCM. Such solutions typically provision a low latency, high bandwidth memory technology for its performance, and then seek to serve most memory accesses from the higher performance memory, only relying on the slower medium if necessary.

Prior work on DRAM-only systems showed the performance superiority of two-tier memory hierarchies, comprising a first tier of 3D stacked DRAM, such as Hynix’ HBM [3] or Micron’s HMC [46], as a high-bandwidth cache and a second tier of planar DRAM

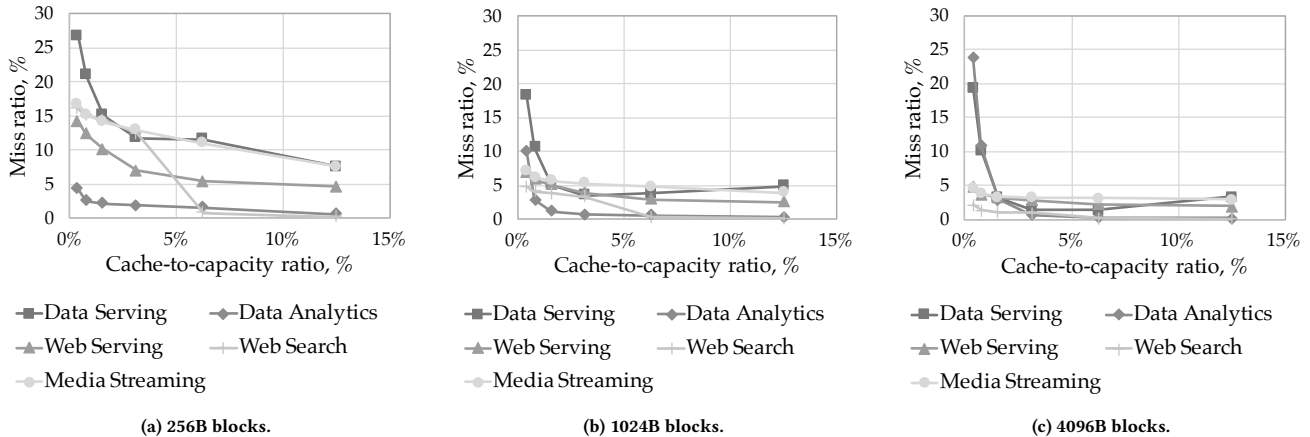


**Figure 5: Miss ratios for a fully associative DRAM cache. The x-axis sweeps through the capacity ratio between the DRAM cache and the backing memory.**

delivering the necessary memory capacity [32, 54, 68]. In our experiments, a two-tier hierarchy with 3D stacked DRAM as a first tier cache, and conventional planar DRAM as a second tier outperforms single-tier planar DRAM by 30%, corroborating prior work [32, 68].

We argue that such a two-tier memory hierarchy is even more applicable to a memory system that includes SCM. Designed correctly, the first tier can serve a large fraction of memory accesses at DRAM latency and thus provide nearly equal performance to a DRAM only system; building the second tier with SCM provides an order of magnitude more capacity at lower cost than using planar DRAM as suggested in prior work.

In the context of building a high-performance and cost-efficient hybrid DRAM-SCM memory hierarchy, proper design of the first-tier 3D stacked DRAM cache (hereafter referred to as a 3D\$) can address the challenges we discussed in §3.1, namely low row buffer hit ratio and increased SCM AMAT. This is the case for two reasons: First, a well designed 3D\$ enables the majority of memory accesses to be serviced at DRAM latency rather than requiring an SCM activation. Second, setting cache block size to be equal to the backing SCM’s row buffer size means that the application’s spatially localized accesses can be aggregated over the block’s relatively long lifetime in the 3D\$; when the block is evicted and written to the backing SCM, a far greater fraction of the row buffer is actually used than if the row was repeatedly opened and closed in the SCM. This access coalescing has the same effect as providing near-ideal access scheduling without the requirements for complex reordering logic, and amortizes the SCM’s latency as we showed is necessary in §2.

Having established the critical advantages of using a 3D\$, we now discuss its design in the next section. We defer a detailed comparison of planar and 3D stacked caches to the evaluation section (§6.3), and a discussion on alternative memory organization approaches, such as flat DRAM-SCM integration, to §8.

### 3.3 3D stacked DRAM cache design

Due to stacked DRAM’s high cost compared to planar DRAM and increased integration complexity, we must be judicious about its architecture and provisioning. There are three main parameters that define a (DRAM) cache’s effectiveness: associativity, capacity, and block size. Prior work studying 3D\$s for server workloads has shown that associativity requirements are modest, with minuscule performance improvements beyond 4 ways [32]. Capacity is a first-order determinant of the cache’s filtering efficiency, while block size introduces a tradeoff between leveraging spatial locality and data overfetch. Prior work on 3D\$s investigated the impact of these parameters for DRAM-based systems [31, 32, 43, 54, 68]. We revisit these key design parameters for 3D\$s in the different context of SCM-based systems, where main memory capacity and access latencies are significantly higher.

To solve the 3D\$ capacity conundrum, we perform an empirical study to investigate whether or not physically feasible 3D\$s can capture the required working sets of our applications. We use a trace simulator based on Flexus [70], and conduct a classical miss ratio study where we sweep the 3D\$’s capacity and search empirically for the “knee of the curve”. We model a fully associative 3D\$ with varied capacity and block sizes, and display the results in Figure 5.

There are two main phenomena that manifest themselves in these results. First, for all of the block sizes shown, a cache provisioned with approximately 2–4% of the backing SCM’s capacity sits at the knee of the curve and therefore represents the sweet spot for provisioning. Recent analysis of Google’s production search code [8] corroborates our findings that a similarly sized cache (the authors evaluated a memory hierarchy with 1–8GB DRAM cache with overall memory capacity of several hundreds of gigabytes) can efficiently accommodate the stack, heap and hot fraction of a multithreaded workload. Such capacity is reasonable even for die-stacked DRAM technologies, as existing products feature capacities up to 8GB, and industry projections expect 64GB by 2020 [6].

Second, we note significantly reduced cache miss ratios with larger 3D\$ block sizes. For example, Web Search’s miss ratio drops

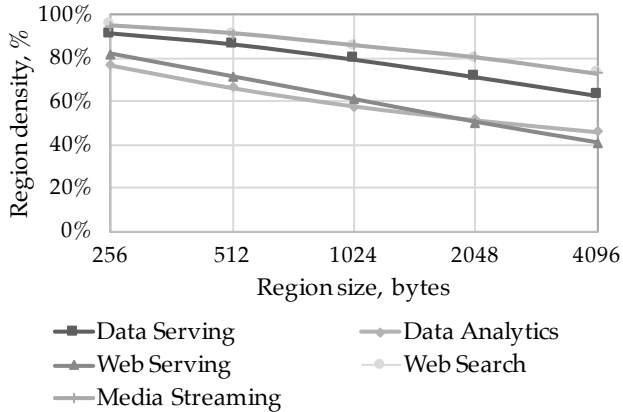


**Figure 6: Percentage of 64B sub-blocks in each DRAM cache block (region size) during its lifetime, measured at first sub-block’s eviction. Note: Web Search and Media Streaming lines overlap.**

from 14.5% to less than 1% as the block size increases from 256B to 4KB. Using larger blocks allows the  $3D\$$  to amortize the cost of accessing the high-latency backing SCM, as every miss now loads larger chunks of data that will likely be accessed in the future. We take these results as further evidence that our set of server workloads exhibits significant spatial locality, but we need a longer temporal window to capture it than the one offered by an open row buffer. The  $3D\$$  serves that exact purpose, coalescing accesses within large blocks of data that, upon eviction, amortize the cost of an SCM row activation and write restoration, as illustrated in §2.

Using terminology commonly used in the literature, we argue that DRAM caches should be architected as *page* caches [34, 40, 68] rather than *block* caches, where the term *page* refers to the cache block size being significantly larger than a typical cache block size of 64B. Page-based caches are superior due to the much lower miss ratios exhibited when the cache block size exceeds 1KB. With a block-based cache, misses to each small block will be serialized once again by the SCM. Existing  $3D\$$  designs that use small blocks, typically equal to the L1 cache block size, are unsuitable for SCM-based memory hierarchies [28, 43, 54, 62]. Using a page-based  $3D\$$  that captures spatial locality harmonizes with our findings in §2, that demonstrate the importance of amortizing long SCM activations with accesses to spatially local data.

We further justify this choice with a direct study on SCM’s latency amortization opportunity as a function of the  $3D\$$ ’s block size. Figure 6 displays the density of regions being evicted from the  $3D\$$  and written to the backing SCM, which we define as the fraction of 64B sub-blocks that are accessed during the region’s lifetime in the cache. All of the workloads exhibit similar behavior, albeit grouped into two different clusters. As the region size increases, density naturally drops. While most of the workloads exhibit densities in excess of 70% between 512B and 2KB region sizes (which correspond to a typical SCM row buffer), Web Serving and Data Analytics have much more sparse traffic patterns, with 15%

less density than the others. Comparing those two workloads to the miss curves in Figure 5, we see that beyond a modest cache size, these same two workloads are the least sensitive to the block size. For cache sizes large enough to hold  $>1\%$  of the dataset, Data Analytics is particularly agnostic to the cache block size, incurring the smallest decrease in miss ratio, due to the fact that it has less innate locality inside each opened row.

By synthesizing the results in Figures 5 and 6, we explicitly argue that the  $3D\$$ ’s block size should match the SCM’s row buffer size. Matching these two parameters allows the  $3D\$$  to coalesce accesses together and therefore amortize the elevated activation and restoration latencies of the backing SCM. Figure 6 essentially shows that the opportunity presented in Figure 3 is attainable, thanks to the combination of the workloads’ innate spatial locality with a page-based  $3D\$$ .

Finally, we present end-to-end application performance results in Figure 7 for a system whose memory hierarchy features a  $3D\$$  sized at 3% of the backing SCM<sup>2</sup>. Performance is normalized to a DRAM-based system featuring the same  $3D\$$  as the SCM-based system. With the exception of Data Serving, the SCM-based system performs better with larger cache block sizes, until an inflection point appears at 2KB blocks. This limitation occurs due to overfetching with 4KB blocks, causing bandwidth contention in the SCM, thus setting an upper bound on the  $3D\$$ ’s block size. Note that the DRAM-based system shows much less sensitivity to the  $3D\$$ ’s block size as a DRAM DIMM’s data array access latency is much closer to the row buffer access latency as compared to an SCM DIMM. In fact, the DRAM-based system is more sensitive to data overfetch (e.g., Data Serving favors the use of relatively small cache blocks in a DRAM-based system), a problem that is partially offset by the higher benefits of row activation amortization in the case of SCM.

Putting all of our observations together, we present three key design guidelines for memory hierarchies that use SCM-backed  $3D\$$ s. First, the performance/cost sweet spot for the  $3D\$$  is approximately 3% of the backing SCM’s size, and it should necessarily feature large blocks (512B–2KB) to capture the spatial locality present in server workloads and amortize the high SCM access latency. We find that for the SCM-backed system, organizing the  $3D\$$  with 2KB blocks hits the sweet spot between hit ratio and bandwidth misuse because of overfetch, while 1KB blocks result in only marginally lower performance.

Second, the SCM’s row buffer size should be the largest permitted by the underlying memory technology, to maximize the potential of latency amortization, up to a maximum of 2KB to avoid data overfetch (Figure 7). If the SCM row buffer is smaller than 2KB because of technology limitations, the  $3D\$$ ’s block size should match the SCM row buffer size, as the latter sets the upper bound for SCM latency amortization.

#### 4 SCM COST/PERFORMANCE TRADEOFF EXPLORATION

In the previous section, we demonstrated that an SCM-based system is able to attain competitive performance with a DRAM-based

<sup>2</sup>Full methodology details available in §5.

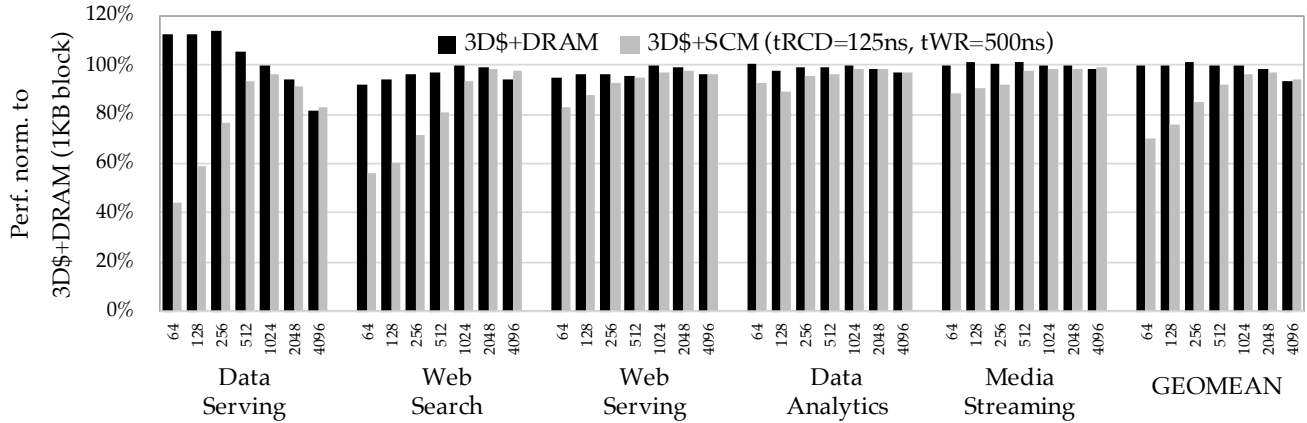


Figure 7: Performance of DRAM-based (black) and SCM-based (gray) systems with the same 3D\$ of variable block size.

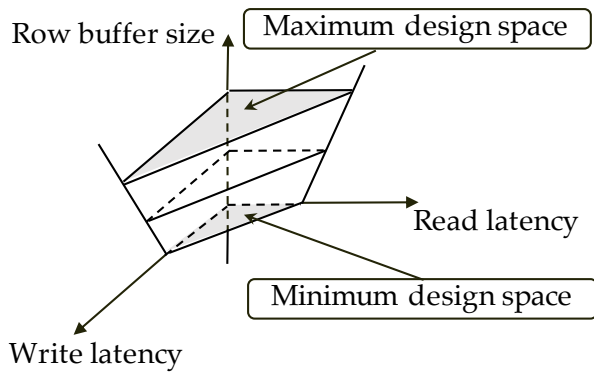


Figure 8: Performance model for SCM design space exploration.

one, with the addition of a 3D\$. However, 3D stacked DRAM technology costs at least an order of magnitude more per bit than SCM, conflicting with the initial motivation of replacing DRAM with SCM as a more cost-efficient memory. Hence, whether the resulting memory hierarchy represents an attractive solution depends on whether the cost reduction from replacing DRAM with SCM offsets the additional cost of a DRAM cache. As SCM itself is a technology that offers a broad spectrum of density/cost/performance operating points, the challenge is to minimize its cost while preserving its performance at acceptable levels. In this section, we trim the broad design space by identifying the key parameters that define SCM’s performance in the context of our memory hierarchy.

In general, the denser the SCM, the lower its cost per bit [45, 53, 63]. We therefore use SCM density as a proxy for SCM cost. Unfortunately, common density optimizations like storing multiple bits per cell or vertical stacking of multiple cell layers result in higher access latency, lower internal bandwidth, and potentially higher read/write disparity [45, 60, 65, 71, 74]. The goal is to deploy the densest (and therefore cheapest) possible SCM while respecting the end-to-end performance goals. Therefore, solving

the cost-performance optimization puzzle requires SCM designers to understand which parameters affect end-to-end performance the most, and by how much.

We identify read latency, write latency, and row buffer size as the three SCM design parameters that control end-to-end application performance. Read latency (i.e., SCM row activation delay) directly affects each memory access’ critical path, while high write latency (i.e., write restoration delay), even though off the critical path, may cause head-of-line blocking delays inside an SCM DIMM [4, 52], implicitly hurting memory access time. Finally, as discussed previously, the row buffer size defines the extent to which SCM’s high access latency can be amortized.

Putting all three parameters together—row buffer size, read latency, and write latency—we devise a three-dimensional SCM design space, illustrated in Figure 8. All the SCM configurations that satisfy the performance target reside inside the volume shaped like a triangular frustum. The SCM devices with the lowest read and write latencies lie close to the vertical axis. All designs for a given row buffer size are represented by a horizontal cut through the frustum, and the resulting plane indicates the space of all read and write latencies that are tolerable with that row buffer size. The frustum’s lower base is defined by the smallest row buffer size that is sufficient to amortize the SCM’s row activations (§3); on that plane, only the fastest SCM devices are acceptable, which are unlikely to deliver the desired high density and low cost. Growing the row buffer size (and implicitly the SCM’s internal bandwidth) widens the design space, as increased amortization opportunity reduces the overall system’s sensitivity to high activation latency.

Given a target domain’s workload characteristics, our methodology helps device designers build a performance model and reason about the feasibility of employing different SCM technologies as main memory. For example, with multi-level cells, designers may deploy smaller serial sensors to optimize for higher density, by sacrificing read latency [74]. Another example is the write latency/bandwidth tradeoff, where designers may choose a different cell writing algorithm, optimizing either for low latency or high bandwidth based on their performance needs. Fewer high-current write iterations result in faster writes, but place an upper limit

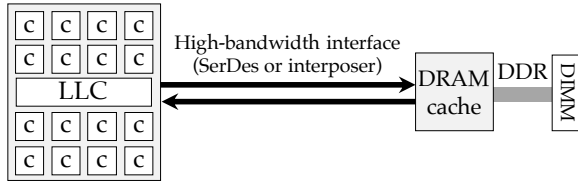


Figure 9: Modeled system overview.

on the row buffer size because of fundamental limitations on the current that can be driven through the data array at any given time [79]. A general observation from our design space exploration is that design planes with bigger row buffers are appealing, as they widen the design space and offer better opportunities for high SCM latency amortization. However, benefiting from such an optimization requires the target application domain’s workloads to exhibit a certain degree of spatial locality.

To summarize, we analyzed three SCM parameters, namely the row buffer size and read/write latencies, and devised a methodology that prunes the vast SCM design space and finds best-fitting solutions for a given application domain. In the following sections, we instantiate this model for our set of representative server workloads and evolve it from qualitative to quantitative, using samples drawn from a wide range of existing SCM configurations. We then use our model to perform a case study of four representative PCM configurations, and compare the performance/cost metric of memory hierarchies built from each configuration.

## 5 EVALUATION METHODOLOGY

In this section, we describe the organization of each system we model throughout the paper, provide the details of our simulation infrastructure, state our performance and cost assumptions, and finally list the parameters we use for our case study with PCM.

**System organization.** Next-generation server processors will feature many cores to exploit the abundant request level parallelism present in online services [23, 44]. Recent server chips follow this very trend: AMD’s Epyc features 32 cores [25] per socket, Qualcomm’s Centriq 48 cores [20], and Phytium’s Mars 64 cores [77]. To make simulation turnaround time tractable, we model a server with 16 cores and a single memory channel, representing a scaled-down version of the OpenCompute server roadmap, which calls for 96 cores and 8 memory channels [48].

We configure the DRAM cache’s size as 3% of the workload’s dataset in order to achieve the cache-to-memory-capacity ratio required for satisfactory performance (see §3.3), unless specified otherwise. We model a 4-way set-associative cache, and for each evaluated configuration, we set the DRAM cache’s block size equal to the SCM’s row buffer size. The DRAM cache is connected to the chip over a high-bandwidth interface (e.g., a SerDes serial link or HBM-like silicon interposer) [3, 30, 46], which in turn is connected to the main memory over a conventional DDR4-2666 channel [47]. A block diagram of our modeled system is displayed in Figure 9.

**Workloads.** Our server workloads are taken from CloudSuite [23]: Data Serving, Web Search, Media Streaming, Data Analytics, and Web Serving. We measure workload performance in User-level IPC (U-IPC), which is defined as the ratio of user instructions committed to the total number of cycles spent in both user and kernel spaces. Prior work [73] has shown U-IPC to be a metric representative of application throughput. We use the rigorous SMARTS sampling methodology [73] to compute all of our performance values using a 95% confidence interval of 5% sample error.

For each workload, we configure the overall memory capacity (i.e., second tier of the hierarchy) to be equal to the workload’s dataset size (i.e., Data Serving, Web Search and Media Streaming have 16GB datasets, while Data Analytics and Web Serving have 32GB datasets). However, today’s datacenter-scale applications can have much larger datasets that even span into the terabyte range [8, 50]; since our work makes specific claims about the capacity ratio relating the two tiers of our memory hierarchy, we conducted a study to verify that our results stand for larger datasets.

To confirm the validity of our results as the dataset size scales up, we analytically studied the relationship between hot and cold data as the entire dataset size increases by orders of magnitude. A key input to these models is a representative query distribution that accurately reflects the skewed popularity phenomenon in datacenter applications. We used the canonical Zipfian distribution, commonly used to rank the frequency of distinct items in a massive dataset [5, 10, 21, 50, 56, 59]. In this experiment, we arbitrarily define the *hot fraction* of the dataset as the subset of data items that absorbs 70% of the accesses.

We studied Zipf coefficients,  $\alpha$ , from 0.6 to 1.01, and observed that while the absolute dataset size scales, the fraction of the dataset classified as hot, decreases. This means that sizing the 3D\$ capacity as a fraction of the total dataset size using a small dataset is conservative, and will accommodate larger datasets with a similar popularity distribution even better. For example, given  $\alpha=0.9$ , scaling a 50 million object dataset by 100-fold leads to a slight decrease of the hot fraction from 5.5% to 4.3% in our analytical model. Therefore, we expect that our scaled down system’s performance is representative of applications with larger datasets, as increasing the absolute size does not significantly affect the disparity between hot and cold data, and actually leads to even higher data locality. This phenomenon would result in a 3D\$ that is an even smaller fraction of the backing memory’s capacity than what we assumed so far.

**Simulation infrastructure.** We use the Flexus [70] full-system cycle-accurate simulator coupled with DRAMSim2 [57]. To extend DRAMSim2 to support non-uniform SCM access latencies, we adjusted its  $t_{RCD}$  and  $t_{WR}$ , and added SCM-related parameters ( $t_{RRDpre}$  and  $t_{RRDact}$ , similarly to the models used by prior work [4, 39]). To simplify our explanations, we refer to the *read* and *write* latencies of the SCM device as  $t_{RCD}$  and  $t_{WR}$ , as they define the major part of the data array’s access.

Without loss of generality, we consider a DRAM cache with tags stored in SRAM [68]. For the DRAM cache’s memory controller, we use a critical-block-first policy and FR-FCFS open-row scheduling with page-based interleaving. We assume that each SCM is packaged in a DIMM form factor. To model different SCM configurations, we replicate expected performance and cost characteristics from



|   |   |
|---|---|
| Cores                                   | ARM Cortex-A72-like; 64-bit, 2.5GHz, OoO, 128-entry ROB, TSO, 3-wide dispatch/retirement  |
| L1 Caches                               | 32KB 2-way L1d, 48KB 3-way L1i, 64-byte blocks, 2 ports, 32 MSHRs, 3-cycle latency (tag+data)                                     |
| LLC                                     | Shared block-interleaved NUCA, 16-way, 4MB total, 1 bank/tile, 8-cycle latency  |
| Coherence                               | Directory-based Non-Inclusive MESI  |
| Interconnect                            | 16x8 crossbar, 16B links, 5 cycles/hop  |
| DRAM cache                              | 4-way, SRAM-based tags, 20ns lookup   |
| Planar                                  | DDR4-2666, 8192B row buffer   |
| 3D stacked (3D\$)                       | SerDes @10GHz, 160Gb/s per direction  |
| $t_{CAS}-t_{RCD}-t_{RP}-t_{RAS}-t_{RC}$ | 14-14-14-24-38  |
| $t_{WR}-t_{WTR}-t_{RTP}-t_{RRD}$        | 9-6-3-3   |
| Main memory                             | 32GB, single memory channel, 2 ranks, 8 x8 banks per rank, Memory controller: 64-entry queue, chan:row:bank:rank:col interleaving |
| Planar DRAM                             | DDR4-2666, 8192B row buffer   |
| $t_{CAS}-t_{RCD}-t_{RP}-t_{RAS}-t_{RC}$ | 14-14-14-24-38  |
| $t_{WR}-t_{WTR}-t_{RTP}-t_{RRD}$        | 9-6-3-3   |
| SCM                                     | DDR4-2666, 512-4096B row buffer   |
| $t_{CAS}-t_{RCD}-t_{RP}-t_{RAS}-t_{RC}$ | 14- $t_{read}$ -14-24- $t_{read}$   |
| $t_{WR}-t_{WTR}-t_{RTP}$                | $t_{write}$ -6-3  |
| $t_{RRDpre}-t_{RRDact}$                 | 2-11  |

**Table 1: System parameters for simulation on Flexus. Timing parameters for all memory technologies shown in ns.**

recent prototypes [36, 60, 71, 72, 83]. For the SCM’s controllers, we model an open-row policy, FR-FCFS scheduling, and page-based interleaving, which is optimized for bulk transfers (§2). We size the write buffer corresponding to the number of banks, with each write entry equal to the page size. Finally, even though existing SCM devices feature row buffers up to 2KB [65], we extend our study to 4KB, which is the largest region we expect to capture semantically significant spatial locality (assuming a 4KB OS page size). Table 1 summarizes our simulation parameters.

## 5.1 Phase-change memory assumptions

PCM is generally considered the most mature SCM technology, as its performance, density and endurance characteristics are well-studied. Additionally, industry has built reliable single-level and multi-level cell (up to 3 bits/cell) configurations. We assume a typical PCM cell and project its performance characteristics for single-level (SLC), multi-level (MLC) and triple-level cells (TLC), which store 1, 2, and 3 bits/cell respectively. For the baseline SLC-PCM configuration, we assume 60ns read latency, and 150ns write latency. Based on a survey of recent PCM prototypes [65], we assume a maximum row buffer size in SLC-PCM of 1024B.

Assuming the same cell material, we project MLC-PCM to operate with 120ns read latency, and a range of possible write latencies, depending on the algorithm used for cell writing. Prior work [79] has described two ways to program an MLC cell. The first approach, which we call  $MLC_{lat}$ , favors faster writes, resulting in write latencies of 550ns and 512B row buffers. The second approach, which we call  $MLC_{BW}$ , favors higher bandwidth,

| Cell configuration | Read lat., ns | Write lat., ns | Total banks/device | Row buffer, bytes | Cost/bit, % |
|--------------------|---------------|----------------|--------------------|-------------------|-------------|
| Planar DRAM        | 14            | 9              | 16                 | 8192              | 100         |
| Stacked DRAM       | 14            | 9              | 256                | 256               | 700         |
| SLC                | 60            | 150            | 16                 | 1024              | 100         |
| $MLC_{lat}$        | 120           | 550            | 16                 | 512               | 50          |
| $MLC_{BW}$         | 120           | 1000           | 16                 | 1024              | 50          |
| TLC                | 250           | 2350           | 16                 | 512               | 25          |

**Table 2: PCM performance and cost characteristics.**

resulting in write latencies of 1000ns and 1024B row buffers. Finally, we project the specifications of TLC-PCM based on a recent industrial prototype [7, 63], and assume read and write latencies of 250ns and 2350ns, respectively. For the row buffer size, we optimistically assume 512B.

**Cost model.** To evaluate the cost of the memory subsystem, we build a model for both planar and 3D stacked DRAM, as well as SCM of different densities. We compare different technologies according to their expected cost/bit metric, normalizing to the same total capacity. Taking planar DRAM’s cost/bit as a baseline, we project 3D stacked DRAM’s cost/bit to be 7x higher than planar DRAM, as cooling and bonding costs increase for stacked dies [15]. We discuss the implications of possible 3D stacked DRAM cost changes over time in §7.

Due to the higher manufacturing costs because of the immaturity of PCM technologies [72, 83], we conservatively assume that the cost/bit of SLC-PCM is equal to commodity planar DRAM. Then, we assume linear cost reduction for MLC and TLC-PCM, proportionally to the number of stored bits per cell (i.e., 50% and 25% cost for 2 and 3 bits/cell). Table 2 summarizes the performance and cost assumptions for all considered technologies: planar DRAM, stacked DRAM, and the four aforementioned PCM configurations (SLC,  $MLC_{lat}$ ,  $MLC_{BW}$ , and TLC).

## 6 EVALUATION

Our methodology seeks to quantify the SCM design space model that we developed in §4, and validate the performance of our proposed memory hierarchy. Using our simulation infrastructure, we study a variety of combinations of row buffer sizes and read/write latencies that we gathered from device datasheets, industry projections, and published literature [7, 45, 63, 65]. We then conduct a case study investigating the feasibility of four different PCM configurations from both performance and cost perspectives, based on the assumptions summarized in Table 2. Finally, we demonstrate that a 3D\$ not only results in better performance but also improved performance/cost as compared to a planar DRAM cache, when used as the first tier of an SCM hierarchy.

### 6.1 Quantifying SCM design space for servers

Figure 10 superimposes a number of different horizontal cuts of Figure 8’s triangular frustum. Each point represents an SCM configuration with different read and write latencies. Each different row buffer size configuration is depicted by a diagonal line that separates the configurations that satisfy the performance target

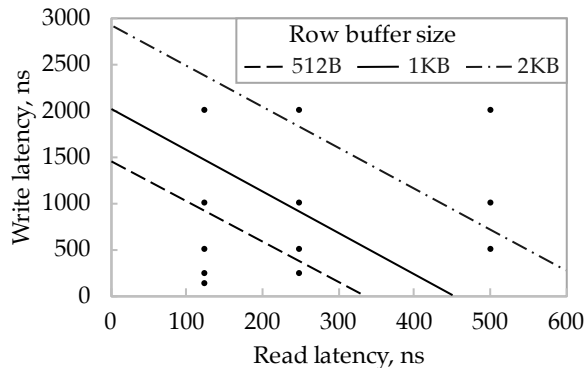


**Figure 10: Performance model for SCM design space evaluation (planar view of design space frustum from above).**

from those that do not (i.e., design points that fall inside or outside the frustum’s volume). Similarly to prior work evaluating emerging technologies in datacenters [1, 24], we set the bound of acceptable performance for the SCM-based memory hierarchy to be within 10% of the best DRAM-based system—which features a 3D\$ with 1KB blocks—for every one of the evaluated workloads.

In Figure 10, the points below each diagonal line satisfy the performance target. For example, with a row buffer size of 512B, the slowest configurations that match the performance target are the skewed SCM configuration with 125ns read and 500ns write latencies, and the symmetric configuration of 250ns read and write latencies.

As we explained in §4, the row buffer size sets the upper bound for SCM access latency amortization, and is therefore the parameter implicitly defining the highest SCM latencies that can be tolerated. Increasing the row buffer size from 512B to 2KB expands the design space linearly. Hence, the maximum read and write latencies meeting our performance target increase proportionally. For example, sweeping the row buffer size from 1KB to 2KB, the maximum acceptable read latency increases from 250ns to 500ns, while the maximum allowed write latency grows from 1 to 2 $\mu$ s. This relation between the maximum allowed latency and row buffer size demonstrates the efficiency of amortizing longer SCM latencies over multiple accesses within a large row buffer.

Application performance turns out to be much less sensitive to slow writes, as compared to reads, because writeback traffic is not directly on the critical path of memory access. This leads us to the important conclusion that SCM’s inherent read/write performance disparity is a secondary concern for hierarchical designs, as a carefully organized 3D\$ collects writes to pages and then drains them to SCM in bulk upon eviction. Accessing the SCM in bulk allows the system to tolerate elevated read and write latencies.

Growing the row buffer and 3D\$’s block size beyond 2KB is not worthwhile, since some applications do not take advantage of the additional data fetched. For example, Data Serving fails to satisfy our performance target using blocks larger than 2KB, even for DRAM-based systems, as we have seen before in Figure 7. For the rest of the workloads, growing the row buffer size to 4KB widens

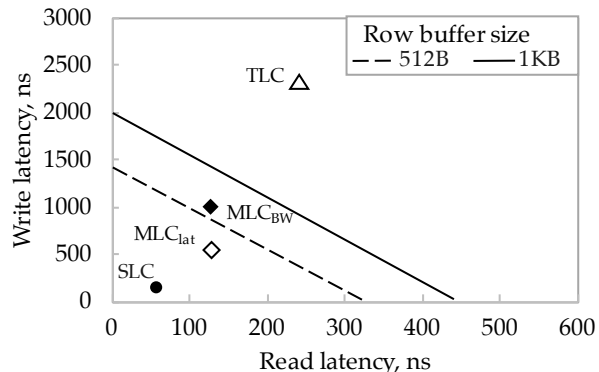


**Figure 11: Performance model for PCM case study (planar view of design space frustum from above).**

the design space further, up to 1 $\mu$ s read and 4 $\mu$ s write latencies (not shown on Figure 10). However, most of the workloads experience performance degradation with cache blocks and row buffers sized at 4KB, as compared to the corresponding 2KB configuration. For example, for the skewed configuration with 125/2000ns read and write latencies, increasing the row buffer from 2KB to 4KB leads to mean performance degradation of 3% and up to 9% for Data Serving. As a result, designers may consider using slower memory with a row buffer size bigger than 2KB only if their applications exhibit that amount of spatial locality.

To summarize, we quantified the frontier that separates plausible SCM configurations from those that are not able to reach the performance target. We demonstrated that a bigger row buffer and corresponding 3D\$ block size widen the SCM design space, albeit without exceeding the spatial locality exhibited by the applications’ access patterns (2KB for our set of server applications). Finally, we make the observation that a simple page-based design efficiently mitigates conventional SCM read/write latency disparity, eliminating the need for any additional disparity-aware mechanisms.

## 6.2 Case study with phase-change memory

We now demonstrate the utility of our performance model by using it to reason about the implications of a number of plausible PCM configurations on overall system performance and cost. We evaluate the economic feasibility of the SLC,  $MLC_{lat}$ ,  $MLC_{BW}$  and TLC PCM configurations we introduced in §5.1.

Figure 11 shows all four configurations as points, according to their assumed read and write latencies. Points with no fill represent configurations with a 512B row buffer, while filled points depict configurations with a 1024B row buffer. Similarly to Figure 10, diagonal lines bound the configurations that match our performance target (within 10% of the best DRAM-based system for each workload), according to their corresponding row buffer sizes. For all the configurations, we model an SCM hierarchy with a page-based 3D\$, sized at 3% of the application dataset, and organized in pages equal to the row buffer size. However, as the TLC-PCM based hierarchy fails to deliver acceptable performance with a 3D\$ sized at 3% of the PCM, we also evaluate TLC-PCM with 6% and 12% 3D\$s, as the low

| Cell configuration     | Perf. geomean | Cache cost | Total memory cost, % | Perf./cost |
|------------------------|---------------|------------|----------------------|------------|
| Planar DRAM            | 1.00          | 0.00       | 1.00                 | 1.00       |
| 3D\$(3%) + DRAM        | 1.31          | 0.22       | 1.22                 | 1.07       |
| 3D\$(3%) + SLC         | 1.30          | 0.22       | 1.22                 | 1.06       |
| 3D\$(3%) + $MLC_{lat}$ | 1.28          | 0.22       | 0.72                 | 1.78       |
| 3D\$(3%) + $MLC_{BW}$  | 1.24          | 0.22       | 0.72                 | 1.72       |
| 3D\$(12%) + TLC        | 1.30          | 0.88       | 1.13                 | 1.15       |

**Table 3: Performance and cost of various memory hierarchies relative to planar DRAM.**

price of TLC-PCM (25% of DRAM) allows us to consider larger 3D\$. Table 3 summarizes the performance results and overall memory hierarchy cost for each PCM technology we considered, normalized to a planar DRAM configuration.

The SLC-PCM configuration we consider attains performance within 2% of the best DRAM configuration with a 3D\$. Although well within our performance target, SLC-PCM’s cost/bit is too high to offset the expense of adding the 3D\$.

For MLC-PCM, we consider two alternatives:  $MLC_{lat}$  and  $MLC_{BW}$ , which are optimized for low write latency and high internal bandwidth respectively. The row buffer sizes of these configurations are 512B and 1KB. According to the model in Figure 11, both configurations deliver performance within the 10% performance target. Although  $MLC_{lat}$  outperforms  $MLC_{BW}$  by 3% on average (1.28 vs. 1.24), designers may prefer  $MLC_{BW}$  as it offers few orders of magnitude higher lifetime [79]. As the cost/bit of MLC-PCMs is half that of planar DRAM, the overall cost and performance/cost metrics improve by 40% and 66% as compared to the DRAM-based system with a 3D\$ of the same capacity (1.78/1.72 vs. 1.07). As compared to planar DRAM, MLC-PCM improves performance/cost by 1.7–1.8 $\times$ , reducing overall memory cost by 28%.

Finally, we consider a TLC-PCM configuration with three different 3D\$, sized at 3%, 6%, and 12% of the dataset. Figure 12 demonstrates that TLC-PCM can only satisfy the performance target with the largest possible 3D\$, which brings the overall memory hierarchy’s cost back in line with the baseline DRAM+3D\$ system. Given its marginal improvement in performance/cost, as well as TLC’s inherently worse endurance [63], we conclude that TLC-PCM is unable to act as a viable main memory technology for server applications. That conclusion is reinforced by the clear superiority of MLC-based alternatives.

In summary, we used our performance/cost model to conduct a case study on four currently offered PCM configurations with different cell densities. We showed that the configuration that stores 2 bits per cell (MLC) drastically improves performance/cost of the memory hierarchy by 1.7 $\times$ , whereas the configurations that store one and three bits per cell (SLC and TLC) are not plausible building blocks for server workloads. Although the real costs of certain memory devices may vary with time, our design exploration methodology still applies, as it relies on fundamental connections among architectural parameters. If the costs of certain technologies change, our model still provides the performance/cost tradeoffs for

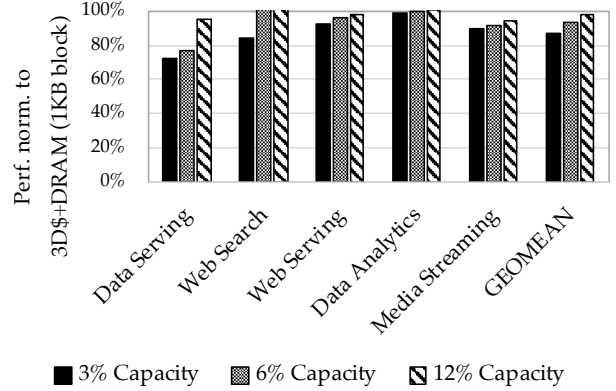


**Figure 12: TLC-PCM performance with 3D\$ of different sizes (SCM:  $t_{RCD}=250ns$ ,  $t_{WR}=2350ns$  as per Table 2).**

the memory devices in question. We elaborate on the implications of potential cost changes in §7.

### 6.3 3D stacked vs. planar DRAM caches

In this section, we specifically show the superiority of a 3D\$ over a planar DRAM alternative as the first level in an SCM memory hierarchy. For this experiment, we use MLC-PCM as the high-capacity tier, and compare 3D stacked DRAM (3D\$) and planar DRAM caches as the high-performance tier. Both cache alternatives are organized with 1KB cache blocks.

Figure 13 shows that using a 3D\$, sized at 3% of the backing SCM device, improves application performance by 31% on average (max 81% for Data Serving) when compared to a single-level DRAM-only configuration. This boost in performance is due to the 3D\$’s ample internal bandwidth and bank-level parallelism. A similarly sized planar DRAM cache fails to meet our performance target of being within 10% of the single-level DRAM-only system for Data Serving and Web Search.

We choose to comment on these two workloads specifically as they represent the cases with the highest memory bandwidth pressure. This pressure is particularly pronounced in a two-tier SCM hierarchy, as it becomes amplified by data movement between the cache tier and backing SCM. The additional evict/fill traffic leads to increased pressure in the memory controller queues of the DRAM cache, and the resulting elevated latencies degrade application performance by up to 16%. The high degree of internal parallelism on 3D stacked caches alleviates this increased pressure.

A four-fold increase of the planar DRAM cache’s capacity (i.e., to 12% of the backing SCM capacity) improves performance by 5%, but has the drawback of diminishing the planar cache’s cost advantage over a 3D\$. As a result, a system with a 3D\$ of a modest (3%) size not only outperforms its alternative with a larger (12%) planar DRAM cache by 33% on average but also delivers 16% better performance/cost. We expect the performance/cost difference between 3D stacked and planar DRAM caches to grow in the future, as 3D\$ solutions pave their way from being exotic HPC products [62] to large-scale deployments in hyperscale datacenters [19, 66].

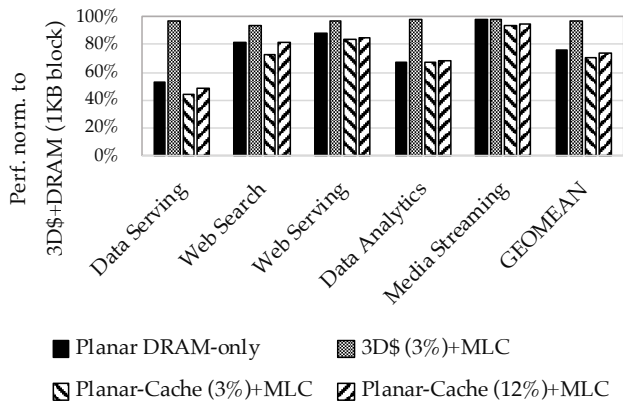


Figure 13: MLC-PCM performance with 3D stacked and planar DRAM caches. (MLC-PCM:  $t_{RCD}=250\text{ns}$ ,  $t_{WR}=2350\text{ns}$ ).

## 7 DISCUSSION

**Sensitivity to SCM and 3D stacked DRAM cost.** Industry has already started to adopt 3D stacked DRAM solutions at a large scale (e.g., TPUv2 [35, 66] is deployed with HBM in Google’s datacenters; Intel and Altera announced their Stratix 10 architecture, with HBM2 on board, aiming at the datacenter and Internet-of-Things markets [19]); at increasingly higher volume, the cost of 3D stacked technology is expected to drop. Cheaper 3D stacked caches will improve the cost effectiveness of our 3D\$+SCM hierarchy, mainly by reducing absolute cost rather than motivating the deployment of larger caches, as we show that they have diminishing performance returns (Figures 5 and 12). Our conclusions regarding the cache block and row buffer sizes required to amortize high SCM latencies only rely on workloads exhibiting spatial locality, and remain unaffected by cost. Significant DRAM cache cost reductions could affect assumptions related to our case studies; e.g., an equivalently priced cache with 4 $\times$  capacity could make TLC-PCM technologies viable.

**SCM persistence aspects.** In this work, we investigated building cost-efficient memory hierarchies for in-memory services, by leveraging emerging high-density SCM technologies. We demonstrated that SCM hierarchies can approach near-DRAM speed, by amortizing high SCM latencies with bulk memory accesses. While we ignored the additional qualitative benefit of persistence, future architectures featuring SCM will likely also leverage the persistence feature for attaining lower-cost durability [9, 42, 49, 80, 81].

To make persistent memory updates durable, the software has to explicitly, and usually synchronously, flush cache lines from the volatile cache hierarchy, which may lead to severe performance degradation. In §2, we demonstrated that fine-grain accesses severely degrade SCM’s internal bandwidth. Using the latency amortization insight, the software should leverage bulk accesses in performance-critical threads, an optimization that can be naturally achieved by using log-based software systems. For example, DudeTM [42] separates performance-critical threads which run

user transactions and generate logs, from background threads that apply updates in-place. As a transactional log entry usually spans a few kilobytes, intelligently written software should be able to amortize the latency cost of writing logs to SCM.

Alternatively, the small 3D\$ can also be made persistent using lithium-ion batteries already available in modern OpenCompute racks [51]. Microsoft practitioners have already demonstrated the maturity of this technology [16, 38], and its ability to reliably back up hundreds of gigabytes of DRAM-resident data upon a power failure; this capacity assumption perfectly matches the 3D\$ capacities we consider in this work. If the 3D\$ is made persistent, then log-generating threads will not need to explicitly use bulk accesses, as their writes can transparently go to the 3D\$ without needing to consider power failures before the logs have been sent to SCM.

## 8 RELATED WORK

Our work draws inspiration from extensive studies in the fields of server architecture and memory systems. In this section, we look at the relationship between our work and prior proposals.

**DRAM caches for servers.** Previous studies have leveraged the wide high speed interface and highly parallel internal structure of 3D\$ to mitigate the “memory bandwidth wall” found in server applications [68]. Block-based organizations [8, 12–14, 28, 43, 54, 62, 76] tend to perform better in the presence of temporal locality, while page-based ones [34, 40, 68] favor applications with spatial locality. Scale-out workloads tend to possess more spatial locality [69] than temporal, motivating the use of page-based caches [68]. However, increasing core counts in servers introduce bandwidth concerns as well, rendering simple page-based designs that overfetch data sub-optimal. The Footprint [32] and Unison [31] cache designs mitigate the overfetch problem, by leveraging an access pattern footprint predictor, at the cost of slightly increasing the DRAM cache miss ratio. Our work extends these observations to SCM hierarchies, and shows that 3D\$s in our context should also be page-based, since transferring data in large chunks amortizes the long latency of accessing SCM. The increased cost of DRAM cache misses in our context does not justify the design decisions of Footprint and Unison cache, which reduce overfetch at the cost of slightly increased miss ratios. Specifically, Footprint cache’s slightly increased miss ratio offsets its lower SCM bandwidth utilization resulting in virtually the same performance as the page-based DRAM cache design, primarily because of its miss traffic’s fine granularity (64B).

Volos et al. [68] also propose a hierarchical memory system for servers, featuring a 3D\$ backed by planar DRAM. Their findings indicate that the 3D\$ should be sized to host 10–15% of the dataset, which is 3–5 $\times$  larger than the 3D\$ we advocate. However, their design goals are different, as they scale down the frequency of the memory bus to DDR-1066 to achieve energy savings. In our work, we assume a commodity DDR4 interface, since SCM DIMMs (adhering to the NVDIMM-P standard) are expected to be DDR4-compliant [61]. The median data rate of DDR4 is DDR-2666 [47], which is significantly higher than that used in previous work [68]. In our setting, a 3D\$ that contains 3% of an application’s dataset is enough to capture most of the available spatial locality (Figure 7) while the second memory tier’s interface offers enough bandwidth

to serve the fraction of traffic that the 3D\$ does not filter. That traffic ends up being slightly higher than the traffic the second memory tier handled by solutions with a 10–15% 3D\$ [68], but is still well within the SCM’s bandwidth capacity.

Other researchers have proposed to mitigate long SCM latencies by using conventional planar DRAM DIMMs for hardware-managed caches [55], OS-based page migration [27] and application-assisted data placement [18]. Applying these designs in the context of server workloads will expose the lack of internal parallelism in planar DRAM devices [68], leading to excess request queuing and therefore latency inflation. Qureshi et al. [55] proposed using a hardware-managed DRAM cache in front of high-capacity SCM to mitigate its high access latency. Our work extends the state of the art with a thorough analysis of server applications’ requirements, demonstrating the superiority of a page-based 3D\$ over its planar and block-based alternatives, and proposing a methodology to help memory architects design the most cost-effective SCM solutions.

**DRAM and SCM flat integration.** While we considered a two-level hierarchy with a hardware-managed DRAM cache as our baseline (§3), a number of prior proposals consider an alternative memory system organization: flat integration of SCM and DRAM on a shared memory bus [1, 18, 27]. In these proposals, software is responsible for managing the data on the heterogeneous DIMMs, relying on heuristics to optimize for performance [1, 18] or energy efficiency [27] by intelligently placing and migrating data between SCM and DRAM. The major strength of this organization is its compatibility with existing memory interfaces and the standard DIMM form factor, that are optimized for fine-grain (64B) data accesses, which, however, turns out to be a weakness as well.

We find that preserving a unified memory interface and using it for heterogeneous memories has two important shortcomings. First, having a unified DDR interface between heterogeneous memories fundamentally limits the headroom for technology-specific optimizations. Specifically, we showed that careful selection of the data transfer granularity (i.e., prioritizing bulk accesses) is essential to mitigate SCM’s much higher access latencies.

Second, because of the expected order-of-magnitude capacity mismatch between SCM and DRAM, it is likely that a workload’s hot dataset fraction won’t fit exclusively in DRAM. For example, Agarwal et al. [1] find that avoiding significant performance degradation (i.e., <3–10%) requires severely limiting demand memory traffic going to the SCM (down to 30–60MB/s) that in turn requires a large fraction (50–70%) of an application’s dataset to be DRAM-resident. Consequently, (i) applications will likely suffer from a shortage of DRAM as well as low utilization of the vast SCM capacity, and (ii) the part of the hot dataset that will end up being directly served from the SCM will be accessed at a fine granularity (64B), giving up on the opportunity for SCM latency amortization via coarse-grained accesses (as we analyzed in §3). In contrast, our proposal of deploying SCM with an appropriately sized page-based 3D\$ will deliver high performance even when the applications’ hot dataset fraction cannot entirely fit in the available DRAM capacity.

Overall, we consider hardware and software mechanisms to be complementary to each other: hardware can provide low latency access for direct demand traffic to the SCM, whereas software can

efficiently optimize data movement across memory channels taking advantage of different high-level characteristics (non-volatility, low static power, high endurance, etc.) of the heterogeneous DIMMs.

**SCM device optimizations.** Since SCM write bandwidth is heavily constrained by current limitations inside the DIMM, industry prototypes have limited-sized row buffers [65]. In order to reduce peak write power, prior work uses a technique called *differential writes*, that detects the subset of bits that actually change their values during a write restoration, which are often as few as 10–15% [39, 55]. This technique shrinks the effective write current and enables greater row buffer sizes, which is critical to our techniques in this paper. Fine-grained power management techniques at the DIMM level have a similar goal but operate above the circuit and cell level [26, 33], and mainly focus on manipulating the limited power budget.

To reduce SCM DIMM latency through the use of SRAM row buffers, Yoon et al. proposed a row buffer locality aware caching policy for heterogeneous memory systems [75], allocating addresses that cause frequent row buffer misses in DRAM. Lee et al. proposed architecting SCM row buffers as small associative structures to leverage temporal locality, meaning that recently closed rows would not be immediately written to the data arrays, but kept in a "backup" row buffer [39]. However, server workloads exhibit poor temporal but abundant spatial locality. Volos et al. [69] proposed proactive data fetch and writeback mechanisms in the on-chip last-level cache, to stream memory traffic in bulk and take advantage of this spatial locality. We also take advantage of spatial locality in server workloads, and design our 3D stacked DRAM cache to capture it with the goal of amortizing bulk transfers to/from our SCM devices.

**Tackling the SCM read/write disparity.** As most SCM technologies show significant disparities in read and write latencies [45, 71, 74], prior work has proposed various mechanisms to mitigate the effects of slow SCM writes. At the application level, researchers have proposed new algorithms that generate less write traffic [11, 67]. At the hardware level, Fedorov et al. [22] augmented a conventional LRU eviction policy to reduce the eviction rate of written data. To mitigate head-of-line blocking of critical reads behind long latency iterative SCM writes, prior work has proposed enhanced request scheduling mechanisms [4, 52, 82], which, for example, cancel or delay writes and allow reads to bypass them. Qureshi et al. [53] proposed a reconfigurable SCM hierarchy that is able to dynamically change its mode of operation between high performance and high capacity. Finally, Sampson et al. [58] proposed using fewer write iterations to improve SCM access latencies at the cost of data precision.

We group this diverse list of prior work together because we obviate the need for any special hardware extensions related to read/write latency disparity. Our SCM hierarchy design methodology helps system designers determine the range of tolerable read/write latency pairs based on the target application domain’s spatial locality characteristics and SCM device’s row buffer size. Furthermore, our insights show that SCM designers can sacrifice device speed to improve other non-performance characteristics. For example, Mellow Writes [78] shows that slowing down writes

can increase the lifetime of ReRAM by orders of magnitude, while Zhang et al. demonstrate a similar tradeoff for PCM [79]. When considering whether or not to adopt such a technique, our performance model provides concrete evidence to architects that extended latencies can indeed be tolerated given the opportunity to amortize them with large row buffers.

## 9 CONCLUSION

The arrival of emerging storage-class memory technologies has the potential to revolutionize datacenter economics, allowing online service providers to deploy servers with far greater capacities at decreased costs. However, directly using SCM as an alternative for DRAM raises significant challenges for server architects, as its higher activation latencies are unacceptable for datacenter applications with strict response time constraints. We show that although fully replacing DRAM with SCM is not possible due to increases in memory access latency, a carefully architected 3D stacked DRAM cache placed in front of the SCM allows the server to match the performance of a state-of-the-art DRAM-based system. The abundant spatial locality present in server applications favors a page based cache organization, which enables amortization of long SCM access latencies.

As SCMs come in a plethora of densities and performance grades, we provide a methodology that helps construct a performance model for a given set of applications, prune the broad design space, and design the most cost efficient memory hierarchy combining a modestly sized 3D stacked DRAM cache architecture with the SCM technology of choice. We demonstrate the utility of our methodology by performing a case study on a number of phase-change memory devices and show that 2-bit cells currently represent the only cost-effective solution for servers.

## REFERENCES

- [1] Neha Agarwal and Thomas F. Wenisch. 2017. Thermostat: Application-transparent Page Management for Two-tiered Main Memory. In *Proceedings of the 22nd International Conference on Architectural Support for Programming Languages and Operating Systems (ASPLOS-XXII)*. 631–644. <https://doi.org/10.1145/3037697.3037706>
- [2] Amazon. 2016. EC2 In-Memory Processing Update: Instances with 4 to 16 TB of Memory + Scale-Out SAP HANA to 34 TB. Available at [aws.amazon.com/blogs/aws/ec2-in-memory-processing-update-instances-with-4-to-16-tb-of-memory-scale-out-sap-hana-to-34-tb](http://aws.amazon.com/blogs/aws/ec2-in-memory-processing-update-instances-with-4-to-16-tb-of-memory-scale-out-sap-hana-to-34-tb).
- [3] AMD. 2016. High Bandwidth Memory, Reinventing Memory Technology. Available at [www.amd.com/en-us/innovations/software-technologies/hbm](http://www.amd.com/en-us/innovations/software-technologies/hbm).
- [4] Mohammad Arjomand, Amin Jadidi, Mahmut T. Kandemir, Anand Sivasubramanian, and Chita R. Das. 2016. MLC PCM main memory with accelerated read. In *Proceedings of the 2016 IEEE International Symposium on Performance Analysis of Systems and Software (ISPASS)*. 143–144.
- [5] Timothy G. Armstrong, Vamsi Ponnkanti, Dhruva Borthakur, and Mark Callaghan. 2013. LinkBench: a database benchmark based on the Facebook social graph. In *SIGMOD Conference*. 1185–1196. <https://doi.org/10.1145/2463676.2465296>
- [6] Arstechnica. 2016. HBM3: Cheaper, up to 64GB on-package, and terabytes-per-second bandwidth. Available at [arstechnica.com/gadgets/2016/08/hbm3-details-price-bandwidth](http://arstechnica.com/gadgets/2016/08/hbm3-details-price-bandwidth).
- [7] Aravinthan Athmanathan. 2016. *Multi-level cell phase-change memory - modeling and reliability framework*. Ph.D. Dissertation. EPFL.
- [8] Grant Ayers, Jung Ho Ahn, Christos Kozyrakis, and Parthasarathy Ranganathan. 2018. Memory Hierarchy for Web Search. In *Proceedings of the 24th IEEE Symposium on High-Performance Computer Architecture (HPCA)*. 643–656.
- [9] Oana Balmau, Rachid Guerraoui, Vasileios Trigonakis, and Igor Zablotchi. 2017. FloDB: Unlocking Memory in Persistent Key-Value Stores. In *Proceedings of the 2017 EuroSys Conference*. 80–94. <https://doi.org/10.1145/3064176.3064193>
- [10] Meeyoung Cha, Haewoon Kwak, Pablo Rodriguez, Yong-Yeol Ahn, and Sue B. Moon. 2007. I tube, you tube, everybody tubes: analyzing the world's largest user generated content video system. In *Proceedings of the 7th ACM SIGCOMM Workshop on Internet Measurement (IMC)*. 1–14. <https://doi.org/10.1145/1298306.1298309>
- [11] Shimin Chen, Phillip B. Gibbons, and Suman Nath. 2011. Rethinking Database Algorithms for Phase Change Memory. In *Proceedings of the 5th Biennial Conference on Innovative Data Systems Research (CIDR)*. 21–31.
- [12] Chia-Chen Chou, Aamer Jaleel, and Moinuddin K. Qureshi. 2014. CAMEO: A Two-Level Memory Organization with Capacity of Main Memory and Flexibility of Hardware-Managed Cache. In *Proceedings of the 47th Annual IEEE/ACM International Symposium on Microarchitecture (MICRO)*. 1–12.
- [13] Chia-Chen Chou, Aamer Jaleel, and Moinuddin K. Qureshi. 2015. BEAR: techniques for mitigating bandwidth bloat in gigascale DRAM caches. In *Proceedings of the 42nd International Symposium on Computer Architecture (ISCA)*. 198–210. <https://doi.org/10.1145/2749469.2750387>
- [14] Chia-Chen Chou, Aamer Jaleel, and Moinuddin K. Qureshi. 2017. BATMAN: techniques for maximizing system bandwidth of memory systems with stacked-DRAM. In *Proceedings of the 3rd International Symposium on Memory Systems (MEMSYS)*. 268–280. <https://doi.org/10.1145/3132402.3132404>
- [15] Xiangyu Dong, Jishen Zhao, and Yuan Xie. 2010. Fabrication Cost Analysis and Cost-Aware Design Space Exploration for 3-D ICs. *IEEE Trans. on CAD of Integrated Circuits and Systems* 29, 12 (2010), 1959–1972.
- [16] Aleksandar Dragojevic, Dushyant Narayanan, Edmund B. Nightingale, Matthew Renzelmann, Alex Shamis, Anirudh Badam, and Miguel Castro. 2015. No compromises: distributed transactions with consistency, availability, and performance. In *Proceedings of the 25th ACM Symposium on Operating Systems Principles (SOSP)*. 54–70. <https://doi.org/10.1145/2815400.2815425>
- [17] DRAMeXchange. 2018. Available at [www.dramexchange.com](http://www.dramexchange.com).
- [18] Subramanya Dulloor, Amitabha Roy, Zheguang Zhao, Narayanan Sundaram, Nadathur Satish, Rajesh Sankaran, Jeff Jackson, and Karsten Schwan. 2016. Data tiering in heterogeneous memory systems. In *Proceedings of the 2016 EuroSys Conference*. 15:1–15:16. <https://doi.org/10.1145/2901318.2901344>
- [19] ExtremeTech. 2017. Intel's new Stratix 10 MX FPGA Taps HBM2 For Massive Memory Bandwidth. Available at [www.altera.com/content/dam/altera-www/global/en\\_US/pdfs/literature/wp/wp-01264-stratix10mx-devices-solve-memory-bandwidth-challenge.pdf](http://www.altera.com/content/dam/altera-www/global/en_US/pdfs/literature/wp/wp-01264-stratix10mx-devices-solve-memory-bandwidth-challenge.pdf).
- [20] ExtremeTech. 2017. Qualcomm announces 48-core Falkor CPUs to run Microsoft Windows Server. Available at [www.extremetech.com/computing/245496-qualcomm-announces-partnership-microsoft-48-core-falkor-cpus-run-windows-server](http://www.extremetech.com/computing/245496-qualcomm-announces-partnership-microsoft-48-core-falkor-cpus-run-windows-server).
- [21] Bin Fan, Hyeontaek Lim, David G. Andersen, and Michael Kaminsky. 2011. Small cache, big effect: provable load balancing for randomly partitioned cluster services. In *Proceedings of the 2011 ACM Symposium on Cloud Computing (SOCC)*. 23. <https://doi.org/10.1145/2038916.2038939>
- [22] Viacheslav V. Fedorov, Sheng Qiu, A. L. Narasimha Reddy, and Paul V. Gratz. 2013. ARI: Adaptive LLC-memory traffic management. *ACM Transactions on Architecture and Code Optimization (TACO)* 10, 4 (2013), 46:1–46:19. <https://doi.org/10.1145/2543697>
- [23] Michael Ferdman, Almutaz Adileh, Yusuf Onur Koçberber, Stavros Volos, Mohammad Alisafae, Djordje Jevdjic, Cansu Kaynak, Adrian Daniel Popescu, Anastasia Ailamaki, and Babak Falsafi. 2012. Clearing the clouds: a study of emerging scale-out workloads on modern hardware. In *Proceedings of the 17th International Conference on Architectural Support for Programming Languages and Operating Systems (ASPLOS-XVII)*. 37–48. <https://doi.org/10.1145/2150976.2150982>
- [24] Peter Xiang Gao, Akshay Narayan, Sagar Karandikar, Joao Carreira, Sangjin Han, Rachit Agarwal, Sylvia Ratnasamy, and Scott Shenker. 2016. Network Requirements for Resource Disaggregation. In *Proceedings of the 12th Symposium on Operating System Design and Implementation (OSDI)*. 249–264.
- [25] Linley Group. 2017. Epyc Relaunches AMD Into Servers. *Microprocessor Report* (June 2017).
- [26] Andrew Hay, Karin Strauss, Timothy Sherwood, Gabriel H. Loh, and Doug Burger. 2011. Preventing PCM banks from seizing too much power. In *Proceedings of the 44th Annual IEEE/ACM International Symposium on Microarchitecture (MICRO)*. 186–195. <https://doi.org/10.1145/2155620.2155642>
- [27] Takahiro Hirofuchi and Ryousei Takano. 2016. RAMinate: Hypervisor-based Virtualization for Hybrid Main Memory Systems. In *Proceedings of the 2016 ACM Symposium on Cloud Computing (SOCC)*. 112–125. <https://doi.org/10.1145/2987550.2987570>
- [28] Cheng-Chieh Huang and Vijay Nagarajan. 2014. ATCache: reducing DRAM cache latency via a small SRAM tag cache. In *Proceedings of the 23rd International Conference on Parallel Architecture and Compilation Techniques (PACT)*. 51–60. <https://doi.org/10.1145/2628071.2628089>
- [29] Intel. 2016. Intel Optane Memory. Available at [www.intel.com/content/www/us/en/architecture-and-technology/optane-memory.html](http://www.intel.com/content/www/us/en/architecture-and-technology/optane-memory.html).
- [30] JEDEC. 2013. Wide I/O 2 Standard. Available at [www.jedec.org/standards-documents/results/jesd229-2](http://www.jedec.org/standards-documents/results/jesd229-2).
- [31] Djordje Jevdjic, Gabriel H. Loh, Cansu Kaynak, and Babak Falsafi. 2014. Unison Cache: A Scalable and Effective Die-Stacked DRAM Cache. In *Proceedings of the 47th Annual IEEE/ACM International Symposium on Microarchitecture (MICRO)*.

- [32] Djordje Jevdjic, Stavros Volos, and Babak Falsafi. 2013. Die-stacked DRAM caches for servers: hit ratio, latency, or bandwidth? Have it all with footprint cache.. In *Proceedings of the 40th International Symposium on Computer Architecture (ISCA)*. 404–415. <https://doi.org/10.1145/2485922.2485957>
- [33] Lei Jiang, Youtao Zhang, Bruce R. Childers, and Jun Yang. 2012. FPB: Fine-grained Power Budgeting to Improve Write Throughput of Multi-level Cell Phase Change Memory.. In *Proceedings of the 45th Annual IEEE/ACM International Symposium on Microarchitecture (MICRO)*. 1–12.
- [34] Xiaowei Jiang, Niti Madan, Li Zhao, Mike Upton, Ravishankar Iyer, Srihari Makeneni, Donald Newell, Yan Solihin, and Rajeev Balasubramonian. 2010. CHOP: Adaptive filter-based DRAM caching for CMP server platforms.. In *Proceedings of the 16th IEEE Symposium on High-Performance Computer Architecture (HPCA)*. 1–12.
- [35] Norman P. Jouppi, Cliff Young, Nishant Patil, David A. Patterson, Gaurav Agrawal, Raminder Bajwa, Sarah Bates, Suresh Bhatia, Nan Boden, Al Borchers, Rick Boyle, Pierre Luc Cantin, Clifford Chao, Chris Clark, Jeremy Coriell, Mike Daley, Matt Dau, Jeffrey Dean, Ben Gelb, Tara Vazir Ghaemmaghami, Rajendra Gottipati, William Gulland, Robert Hagmann, C. Richard Ho, Doug Hogberg, John Hu, Robert Hundt, Dan Hurt, Julian Ibarz, Aaron Jaffey, Alek Jaworski, Alexander Kaplan, Harshit Khaitan, Daniel Killebrew, Andy Koch, Naveen Kumar, Steve Lacy, James Laudon, James Law, Diemthu Le, Chris Leary, Zhuyuan Liu, Kyle Lucke, Alan Lundin, Gordon MacKean, Adriana Maggiore, Maire Mahony, Kieran Miller, Rahul Nagarajan, Ravi Narayanaswami, Ray Ni, Kathy Nix, Thomas Norrie, Mark Omernick, Narayana Penukonda, Andy Phelps, Jonathan Ross, Matt Ross, Amir Salek, Emad Samadiani, Chris Severn, Gregory Sizikov, Matthew Snellman, Jed Souter, Dan Steinberg, Andy Swing, Mercedes Tan, Gregory Thorson, Bo Tian, Horia Toma, Erick Tuttle, Vijay Vasudevan, Richard Walter, Walter Wang, Eric Wilcox, and Doe Hyun Yoon. 2017. In-Datacenter Performance Analysis of a Tensor Processing Unit.. In *Proceedings of the 44th International Symposium on Computer Architecture (ISCA)*. 1–12. <https://doi.org/10.1145/3079856.3080246>
- [36] Gosia Jarczak. 2015. Advances and Trends of RRAM technology. Available at [www.semicon.taiwan.org/en/sites/semicon.taiwan.org/files/data15/docs/2\\_5\\_5\\_advances\\_and\\_trends\\_in\\_rram\\_technology\\_semicon\\_taiwan\\_2015\\_final.pdf](http://www.semicon.taiwan.org/en/sites/semicon.taiwan.org/files/data15/docs/2_5_5_advances_and_trends_in_rram_technology_semicon_taiwan_2015_final.pdf).
- [37] Svilen Kanev, Juan Pablo Darago, Kim M. Hazelwood, Parthasarathy Ranganathan, Tipp Moseley, Gu-Yeon Wei, and David M. Brooks. 2015. Profiling a warehouse-scale computer.. In *Proceedings of the 42nd International Symposium on Computer Architecture (ISCA)*. 158–169. <https://doi.org/10.1145/2749469.2750392>
- [38] Rajat Kateja, Anirudh Badam, Sriram Govindan, Bikash Sharma, and Greg Ganger. 2017. Viyojit: Decoupling Battery and DRAM Capacities for Battery-Backed DRAM.. In *Proceedings of the 44th International Symposium on Computer Architecture (ISCA)*. 613–626. <https://doi.org/10.1145/3079856.3080236>
- [39] Benjamin C. Lee, Engin Ipek, Onur Mutlu, and Doug Burger. 2009. Architecting phase change memory as a scalable dram alternative.. In *Proceedings of the 36th International Symposium on Computer Architecture (ISCA)*. 2–13. <https://doi.org/10.1145/1555754.1555758>
- [40] Yongjun Lee, Jongwon Kim, Hakbeom Jang, Hyunggyun Yang, Jangwoo Kim, Jinkyu Jeong, and Jae W. Lee. 2015. A fully associative, tagless DRAM cache.. In *Proceedings of the 42nd International Symposium on Computer Architecture (ISCA)*. 211–222. <https://doi.org/10.1145/2749469.2750383>
- [41] Linley Group. 2015. 3D XPoint Fetches Data in a Flash. *Microprocessor Report* (September 2015).
- [42] Mengxing Liu, Mingxing Zhang, Kang Chen, Xuehai Qian, Yongwei Wu, Weimin Zheng, and Jinglei Ren. 2017. DudeTM: Building Durable Transactions with Decoupling for Persistent Memory.. In *Proceedings of the 22nd International Conference on Architectural Support for Programming Languages and Operating Systems (ASPLOS-XXII)*. 329–343. <https://doi.org/10.1145/3037697.3037714>
- [43] Gabriel H. Loh and Mark D. Hill. 2011. Efficiently enabling conventional block sizes for very large die-stacked DRAM caches.. In *Proceedings of the 44th Annual IEEE/ACM International Symposium on Microarchitecture (MICRO)*. 454–464. <https://doi.org/10.1145/2155620.2155673>
- [44] Pejman Lotfi-Kamran, Boris Grot, Michael Ferdman, Stavros Volos, Yusuf Onur Koçberber, Javier Picorel, Almutaz Adileh, Djordje Jevdjic, Sachin Idgunji, Emre Özer, and Babak Falsafi. 2012. Scale-out processors.. In *Proceedings of the 39th International Symposium on Computer Architecture (ISCA)*. 500–511.
- [45] Darsen Lu. 2016. Tutorial on Emerging Memory Devices. Available at [people.oregonstate.edu/~slu/Micro\\_MT/presentations/micro16\\_emerging\\_mem\\_tutorial\\_darsen.pdf](http://people.oregonstate.edu/~slu/Micro_MT/presentations/micro16_emerging_mem_tutorial_darsen.pdf).
- [46] Micron Technology Inc. 2014. Hybrid Memory Cube Second Generation. Available at [investors.micron.com/releasedetail.cfm?ReleaseID=828028](http://investors.micron.com/releasedetail.cfm?ReleaseID=828028).
- [47] Micron Technology Inc. 2018. DDR4 SDRAM Datasheets. Available at [www.micron.com/products/dram/ddr4-sdram](http://www.micron.com/products/dram/ddr4-sdram).
- [48] Microsoft. 2016. Open CloudServer OCS V2.1 Specification. Available at [www.opencompute.org/wiki/Server/SpecsAndDesigns](http://www.opencompute.org/wiki/Server/SpecsAndDesigns).
- [49] Sanketh Nalli, Swapnil Haria, Mark D. Hill, Michael M. Swift, Haris Volos, and Kimberly Keeton. 2017. An Analysis of Persistent Memory Use with WHISPER.. In *Proceedings of the 22nd International Conference on Architectural Support for Programming Languages and Operating Systems (ASPLOS-XXII)*. 135–148. <https://doi.org/10.1145/3037697.3037730>
- [50] Stanko Novakovic, Alexandros Daglis, Edouard Bugnion, Babak Falsafi, and Boris Grot. 2016. The Case for RackOut: Scalable Data Serving Using Rack-Scale Systems.. In *Proceedings of the 2016 ACM Symposium on Cloud Computing (SOCC)*. 182–195. <https://doi.org/10.1145/2987550.2987577>
- [51] Open Compute Project. 2017. Open Rack Standard v2.0. Available at [www.opencompute.org/wiki/Open\\_Rack/SpecsAndDesigns](http://www.opencompute.org/wiki/Open_Rack/SpecsAndDesigns).
- [52] Moinuddin K. Qureshi, Michele Franceschini, and Luis Alfonso Lastras-Montano. 2010. Improving read performance of Phase Change Memories via Write Cancellation and Write Pausing.. In *Proceedings of the 16th IEEE Symposium on High-Performance Computer Architecture (HPCA)*. 1–11. <https://doi.org/10.1109/HPCA.2010.5416645>
- [53] Moinuddin K. Qureshi, Michele Franceschini, Luis Alfonso Lastras-Montano, and John P. Karidis. 2010. Morphable memory system: a robust architecture for exploiting multi-level phase change memories.. In *Proceedings of the 37th International Symposium on Computer Architecture (ISCA)*. 153–162. <https://doi.org/10.1145/1815961.1815981>
- [54] Moinuddin K. Qureshi and Gabriel H. Loh. 2012. Fundamental latency trade-off in architecting DRAM caches: Outperforming impractical SRAM-tags with a simple and practical design.. In *Proceedings of the 45th Annual IEEE/ACM International Symposium on Microarchitecture (MICRO)*. 235–246. <https://doi.org/10.1109/MICRO.2012.30>
- [55] Moinuddin K. Qureshi, Vijayalakshmi Srinivasan, and Jude A. Rivers. 2009. Scalable high performance main memory system using phase-change memory technology.. In *Proceedings of the 36th International Symposium on Computer Architecture (ISCA)*. 24–33. <https://doi.org/10.1145/1555754.1555760>
- [56] Venugopalan Ramasubramanian and Emin Gün Sirer. 2004. Beehive: O(1) Lookup Performance for Power-Law Query Distributions in Peer-to-Peer Overlays.. In *Proceedings of the 1st Symposium on Networked Systems Design and Implementation (NSDI)*. 99–112.
- [57] Paul Rosenfeld, Elliott Cooper-Balis, and Bruce Jacob. 2011. DRAMSim2: A Cycle Accurate Memory System Simulator. *Computer Architecture Letters* 10, 1 (2011), 16–19. <https://doi.org/10.1109/L-CA.2011.4>
- [58] Adrian Sampson, Jacob Nelson, Karin Strauss, and Luis Ceze. 2013. Approximate storage in solid-state memories.. In *Proceedings of the 46th Annual IEEE/ACM International Symposium on Microarchitecture (MICRO)*. 25–36. <https://doi.org/10.1145/2540708.2540712>
- [59] Navin Sharma, Sean Kenneth Barker, David E. Irwin, and Prashant J. Shenoy. 2011. Blink: managing server clusters on intermittent power.. In *Proceedings of the 16th International Conference on Architectural Support for Programming Languages and Operating Systems (ASPLOS-XVI)*. 185–198. <https://doi.org/10.1145/1950365.1950389>
- [60] Siva Sivaram. 2016. Storage Class Memory: Learning from 3D NAND. Available at [www.flashmemorysummit.com/English/Collaterals/Proceedings/2016/20160809\\_Keynote4\\_WD\\_Sivaram.pdf](http://www.flashmemorysummit.com/English/Collaterals/Proceedings/2016/20160809_Keynote4_WD_Sivaram.pdf).
- [61] SNIA. 2016. NVDIMM - changes are here so what's next. Available at [www.snia.org/sites/default/files/SSSI/NVDIMM%20-%20Changes%20are%20Here%20So%20What's%20Next%20-%20final.pdf](http://www.snia.org/sites/default/files/SSSI/NVDIMM%20-%20Changes%20are%20Here%20So%20What's%20Next%20-%20final.pdf).
- [62] Avinash Sodani, Roger Gramunt, Jesus Corbal, Ho-Seop Kim, Krishna Vinod, Sundaram Chinthamani, Steven Hutsell, Rajat Agarwal, and Yen-Chen Liu. 2016. Knights Landing: Second-Generation Intel Xeon Phi Product. *IEEE Micro* 36, 2 (2016), 34–46.
- [63] Milos Stanisavljevic, Haris Pozidis, Aravinthan Athmanathan, Nikolaos Papan-dreou, Thomas Mittelholzer, and Evangelos Eleftheriou. 2016. Demonstration of reliable triple-level-cell (TLC) phase-change memory. In *Memory Workshop (IMW), 2016 IEEE 8th International*. IEEE, 1–4.
- [64] Jeffrey Stuecheli, Dimitris Kaseridis, David Daly, Hillery C. Hunter, and Lizy K. John. 2010. The virtual write queue: coordinating DRAM and last-level cache policies.. In *Proceedings of the 37th International Symposium on Computer Architecture (ISCA)*. 72–82. <https://doi.org/10.1145/1815961.1815972>
- [65] Kosuke Suzuki and Steven Swanson. 2015. *The Non-Volatile Memory Technology Database (NVMDB)*. Technical Report CS2015-1011. Department of Computer Science & Engineering, University of California, San Diego. <http://nvmdb.ucsd.edu>
- [66] Tom's Hardware. 2017. Hot Chips 2017: A Closer Look At Google's TPU v2. Available at [www.tomshardware.com/news/tpu-v2-google-machine-learning,35370.html](http://www.tomshardware.com/news/tpu-v2-google-machine-learning,35370.html).
- [67] Stratis Viglas. 2014. Write-limited sorts and joins for persistent memory. *PVLDB* 7, 5 (2014), 413–424.
- [68] Stavros Volos, Djordje Jevdjic, Babak Falsafi, and Boris Grot. 2017. Fat caches for scale-out servers. *IEEE Micro* 37, 2 (2017), 90–103.
- [69] Stavros Volos, Javier Picorel, Babak Falsafi, and Boris Grot. 2014. BuMP: Bulk Memory Access Prediction and Streaming.. In *Proceedings of the 47th Annual IEEE/ACM International Symposium on Microarchitecture (MICRO)*. 545–557.
- [70] Thomas F. Wenisch, Roland E. Wunderlich, Michael Ferdman, Anastassia Ailamaki, Babak Falsafi, and James C. Hoe. 2006. SimFlex: Statistical Sampling of Computer System Simulation. *IEEE Micro* 26, 4 (2006), 18–31.
- [71] HSP Wong, C. Ahn, J. Cao, H.Y. Chen, S.W. Fong, Z. Jiang, C. Neumann, S. Qin, J. Sohn, Y. Wu, et al. 2016. *Stanford memory trends*. Technical Report. Stanford

University.

- [72] Computer World. 2016. FAQ: 3D XPoint memory, NAND flash killer or DRAM replacement? Available at [www.computerworld.com/article/3194147/data-storage/faq-3d-xpoint-memory-nand-flash-killer-or-dram-replacement.html](http://www.computerworld.com/article/3194147/data-storage/faq-3d-xpoint-memory-nand-flash-killer-or-dram-replacement.html).
- [73] Roland E. Wunderlich, Thomas F. Wenisch, Babak Falsafi, and James C. Hoe. 2003. SMARTS: Accelerating Microarchitecture Simulation via Rigorous Statistical Sampling. In *Proceedings of the 30th International Symposium on Computer Architecture (ISCA)*. 84–95.
- [74] Cong Xu, Dimin Niu, Naveen Muralimanohar, Norman P Jouppi, and Yuan Xie. 2013. Understanding the trade-offs in multi-level cell ReRAM memory design. In *Proceedings of the 50th ACM/EDAC/IEEE Design Automation Conference (DAC)*. IEEE, 1–6.
- [75] HanBin Yoon, Justin Meza, Rachata Ausavarungnirun, Rachael Harding, and Onur Mutlu. 2012. Row buffer locality aware caching policies for hybrid memories. In *Proceedings of the 30th International IEEE Conference on Computer Design (ICCD)*. 337–344.
- [76] Vinson Young, Prashant J. Nair, and Moinuddin K. Qureshi. 2017. DICE: Compressing DRAM Caches for Bandwidth and Capacity. In *Proceedings of the 44th International Symposium on Computer Architecture (ISCA)*. 627–638. <https://doi.org/10.1145/3079856.3080243>
- [77] Charles Zhang. 2015. Mars: A 64-core ARMv8 processor. *Hot Chips Symposium*.
- [78] Lunkai Zhang, Brian Neely, Diana Franklin, Dmitri B. Strukov, Yuan Xie, and Frederic T. Chong. 2016. Mellow Writes: Extending Lifetime in Resistive Memories through Selective Slow Write Backs. In *Proceedings of the 43rd International Symposium on Computer Architecture (ISCA)*. 519–531.
- [79] Mingzhe Zhang, Lunkai Zhang, Lei Jiang, Zhiyong Liu, and Frederic T. Chong. 2017. Balancing Performance and Lifetime of MLC PCM by Using a Region Retention Monitor. In *Proceedings of the 23rd IEEE Symposium on High-Performance Computer Architecture (HPCA)*. 385–396.
- [80] Yiyang Zhang and Steven Swanson. 2015. A study of application performance with non-volatile main memory. In *Proceedings of the 31st Symposium on Mass Storage Systems and Technologies (MSST)*. 1–10.
- [81] Yiyang Zhang, Jian Yang, Amirsaman Memaripour, and Steven Swanson. 2015. Mojim: A Reliable and Highly-Available Non-Volatile Memory System. In *Proceedings of the 20th International Conference on Architectural Support for Programming Languages and Operating Systems (ASPLOS-XX)*. 3–18. <https://doi.org/10.1145/2694344.2694370>
- [82] Jishen Zhao, Onur Mutlu, and Yuan Xie. 2014. FIRM: Fair and High-Performance Memory Control for Persistent Memory Systems. In *Proceedings of the 47th Annual IEEE/ACM International Symposium on Microarchitecture (MICRO)*. 153–165.
- [83] Yanqi Zhou, Ramnatthan Alagappan, Amirsaman Memaripour, and Anirudh Badam David Wentzlaff. 2017. *HNVN: Hybrid nvm enabled datacenter design and optimization*. Technical Report. Microsoft Research.